

See discussions, stats, and author profiles for this publication at: <https://www.researchgate.net/publication/228501063>

# Electron Affinities of Selected Hydrogenated Silicon Clusters ( $\text{Si}_x\text{H}_y$ , $x=1-7$ , $y=0-15$ ) from Density Functional Theory Calculations

ARTICLE *in* THE JOURNAL OF PHYSICAL CHEMISTRY A · JUNE 2000

Impact Factor: 2.69 · DOI: 10.1021/jp000626b

---

CITATIONS

20

---

READS

19

## 1 AUTHOR:



Mark Swihart

University at Buffalo, The State University of ...

213 PUBLICATIONS 6,122 CITATIONS

SEE PROFILE

# Electron Affinities of Selected Hydrogenated Silicon Clusters ( $\text{Si}_x\text{H}_y$ , $x = 1-7$ , $y = 0-15$ ) from Density Functional Theory Calculations

Mark T. Swihart<sup>†</sup>

Department of Chemical Engineering, The University at Buffalo (SUNY), Buffalo, New York 14260-4200

Received: February 17, 2000; In Final Form: April 19, 2000

Adiabatic electron affinities for 72 hydrogenated silicon compounds containing up to seven silicon atoms are presented. These were computed using density functional theory at the B3LYP/6-311+G(3df,2p)//B3LYP/6-31G(d) level and are expected to be accurate to within about 0.15 eV. The electron affinities for acyclic silyl radicals, silylenes, and silenes were all found to increase smoothly with increasing molecular size. Electron affinities of the silyl radicals were greater than those of the silylenes, which were, in turn, greater than those of the silenes. The electron affinity increased with silyl substitution for hydrogen at the unsaturated site for all three of these classes of compounds. Some cyclic and polycyclic clusters had electron affinities that deviated significantly from the trends observed for the acyclic compounds. These deviations could be rationalized (a) in terms of differences in ring strain between the neutral and anionic species and (b) in terms of differences in the interactions between nonbonding electrons and other atoms between the neutral and anionic species.

## Introduction

The formation of particles in silane plasmas is of wide technological interest because of the extensive use of these plasmas in microelectronics processing, and the deleterious effect of particle formation on these processes. As a result, intense research on nanoparticle formation in these systems has been conducted over the past decade. However, the mechanisms of particle nucleation and growth are still not well understood, and the ability to quantitatively model particle formation is lacking. Recently, detailed chemical kinetic models of the formation of hydrogenated silicon clusters in both thermal<sup>1,2</sup> and plasma<sup>3</sup> systems have been presented. In silane discharges, most of the hydrogenated silicon clusters containing more than one silicon atom are either neutral or negatively charged. Data on the electron affinities of these hydrogenated silicon clusters are therefore a key component of these kinetic models of particle nucleation in silane plasma systems.

Few values of electron affinities of hydrogenated silicon compounds are available. Electron affinities of  $\text{SiH}_3$ ,  $\text{SiH}_2$ ,  $\text{SiH}$ , and  $(\text{Si})_n$ ,  $n = 1-12$  have been determined experimentally. These values, along with estimates for a few additional compounds, can be found in the review by Perrin et al.<sup>4</sup> Electron affinities of a few other small hydrogenated silicon compounds have been studied using electronic structure calculations. Most of these computational results, as well as a good discussion of the difficulties involved in calculating electron affinities using ab initio methods, can be found in the review by Kalcher and Sax.<sup>5</sup> Damrauer and Hankin have also reviewed the thermochemistry of silicon-containing anions in the gas phase.<sup>6</sup> To our knowledge, there has been no previous systematic study of electron affinities of silicon–hydrogen compounds that includes the larger clusters whose formation can lead to nucleation of nanoparticles.

Saturated silanes, such as  $\text{SiH}_4$ ,  $\text{Si}_2\text{H}_6$ , etc., in general have negative electron affinities. That is, they do not form thermodynamically stable anions in the gas phase. We have therefore primarily considered unsaturated silicon species in this study.

The majority of the selected hydrogenated silicon clusters are the silyl radicals, silylene biradicals, and nominally doubly bonded silene species that were included in the kinetic models of particle formation presented by Swihart et al.<sup>2</sup> and Kortshagen et al.<sup>3</sup> These clusters were selected on the basis of the expectation that each is the most thermodynamically stable isomer of its particular chemical type. That is, for the stoichiometry  $\text{Si}_x\text{H}_{2y}$ , we consider the most stable silylene isomer and the most stable silene isomer. For the stoichiometry  $\text{Si}_x\text{H}_{2y+1}$  we consider the most stable silyl radical. All acyclic structural isomers of the three- and four-silicon-containing molecules, as well as a few additional isomers of the larger compounds have also been included to help elucidate the relationships between molecular structure and electron affinity. Figure 1 shows sketches of the selected isomers. Adiabatic electron affinities, computed as the difference between the energy of the anion and the neutral at their respective minimum energy geometries, are presented for these clusters containing up to seven silicon atoms.

## Methodology

The adiabatic electron affinities presented here were calculated as the difference between the energy of the neutral and the energy of the anion, including zero-point energy, at their respective minimum energy geometries. All calculations used density functional theory with the B3LYP functional. This functional employs Becke's gradient-corrected exchange functional,<sup>7</sup> the Lee–Yang–Parr correlational functional,<sup>8</sup> and three parameters fit to the original G2 test set.<sup>9</sup> The geometry optimizations and frequency calculations used the 6-31G(d) basis set. The energy at that geometry was then calculated using the 6-311+G(3df,2p) basis set. For computing the zero-point energies, the vibrational frequencies at the B3LYP/6-31G(d) level were scaled by 0.9613, as recommended by Wong.<sup>10</sup> All of the calculations presented here were carried out using Gaussian94.<sup>11</sup>

Curtiss et al.<sup>12</sup> have presented an assessment of density functional theory calculations for computing electron affinities. They compared results using seven different functionals for 58 atoms and small molecules with known electron affinities. They used the same basis set (6-311+G(3df,2p)) as has been used

<sup>†</sup> E-mail: swihart@eng.buffalo.edu.

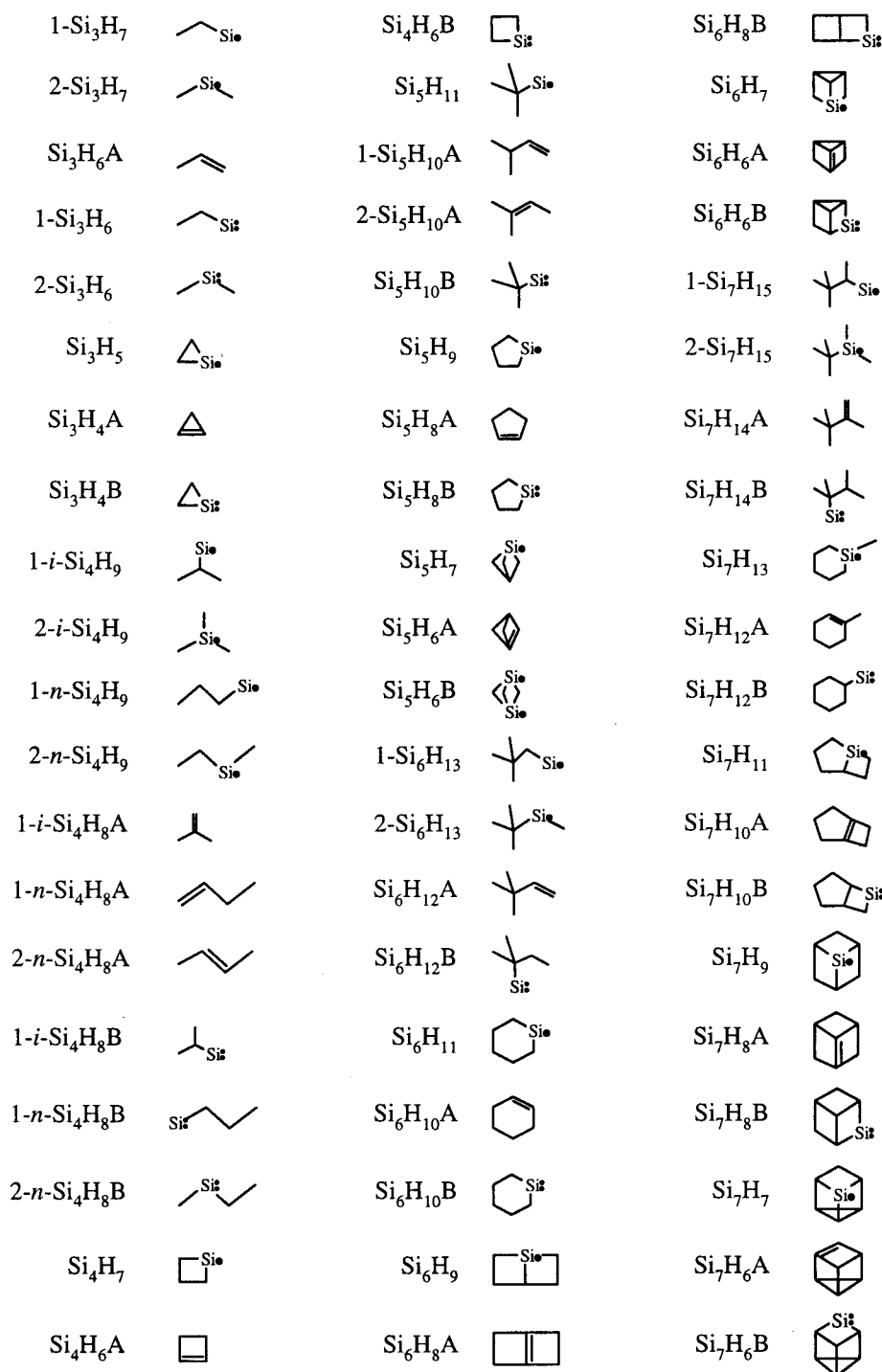


**Figure 1.** Structural sketches of molecules containing three or more silicon atoms. Structures shown are intended to indicate only the connectivity of the atoms and are not intended to illustrate the detailed geometry of the species. The suffix A is used to indicate a silene, and the suffix B is used to indicate a silylene (with the exception of Si<sub>5</sub>H<sub>6</sub>B, which is a diradical, as shown above).

here for the energy calculations, but optimized the geometries at the MP2(full)/6-31G(d) level rather than the B3LYP/6-31G(d) level used here. They found an average absolute deviation of 0.131 eV between calculation and experiment for their results using the B3LYP functional. In their calculations, the electron affinity was more likely to be overpredicted than underpredicted. The average deviation (experiment minus theory) for calculations using the B3LYP functional was -0.087 eV. On the basis of their results, we can reasonably expect the electron affinities computed here to be accurate to within about one-tenth of an electronvolt. Compound methods, such as the G2 method, can provide more accurate calculations of electron affinities<sup>12</sup> but

are too computationally expensive to apply to the larger clusters considered here, which contain up to seven heavy atoms and up to 114 total electrons.

## Results and Discussion

The computed total energies for the neutral and anionic species, along with the adiabatic electron affinities calculated from those energies, are presented in Table 1. The computed geometries and vibrational frequencies are not presented but may be obtained from the author upon request. For the species containing an even number of hydrogen atoms, both silylene and silene isomers were considered. In Table 1 and Figure 1,

TABLE 1: Computed Energies and Electron Affinities

species	total energy (hartrees) <sup>a</sup>		electron affinity (eV)		species	total energy (hartrees) <sup>a</sup>		electron affinity (eV)
	neutral	anion	this work	experiment <sup>b</sup>		neutral	anion	
Si	-289.39449	-289.44293	1.32	1.39	Si <sub>5</sub> H <sub>10</sub> B	-1453.48970	-1453.56631	2.08
SiH	-290.01139	-290.05735	1.25	1.28	Si <sub>5</sub> H <sub>9</sub>	-1452.92288	-1453.00895	2.34
SiH <sub>2</sub>	-290.63218	-290.67487	1.16	1.12	Si <sub>5</sub> H <sub>8</sub> A	-1452.32457	-1452.38397	1.62
SiH <sub>3</sub>	-291.24420	-291.29587	1.41	1.41	Si <sub>5</sub> H <sub>8</sub> B	-1452.30917	-1452.39062	2.22
SiH <sub>4</sub>	-291.88830	-291.84064	-1.30		Si <sub>5</sub> H <sub>7</sub>	-1451.71459	-1451.80882	2.56
Si <sub>2</sub>	-578.90078	-578.97761	2.09	2.20	Si <sub>5</sub> H <sub>6</sub> A	-1451.10309	-1451.17561	1.97
SiHSi	-579.52181	-579.60159	2.17		Si <sub>5</sub> H <sub>6</sub> B	-1451.14320	-1451.19975	1.54
SiSiH	-579.50662	-579.58674	2.18		1-Si <sub>6</sub> H <sub>13</sub>	-1744.81437	-1744.89700	2.25
H <sub>2</sub> SiSiH <sub>2</sub>	-581.35393	-581.40191	1.31		2-Si <sub>6</sub> H <sub>13</sub>	-1744.81851	-1744.90757	2.42
H <sub>3</sub> SiSiH	-581.34478	-581.40632	1.67		Si <sub>6</sub> H <sub>12</sub> A	-1744.21313	-1744.27934	1.80
H <sub>3</sub> SiSiH <sub>2</sub>	-581.95953	-582.02633	1.82		Si <sub>6</sub> H <sub>12</sub> B	-1744.20208	-1744.28061	2.14
H <sub>3</sub> SiSiH <sub>3</sub>	-582.59898	-582.58307	-0.43		Si <sub>6</sub> H <sub>11</sub>	-1743.64086	-1743.72844	2.38
1-Si <sub>3</sub> H <sub>7</sub>	-872.67098	-872.74312	1.96		Si <sub>6</sub> H <sub>10</sub> A	-1743.03915	-1743.10421	1.77
2-Si <sub>3</sub> H <sub>7</sub>	-872.67621	-872.75406	2.12		Si <sub>6</sub> H <sub>10</sub> B	-1743.02601	-1743.11054	2.30
Si <sub>3</sub> H <sub>6</sub> A	-872.07123	-872.12684	1.51		Si <sub>6</sub> H <sub>9</sub>	-1742.43342	-1742.52204	2.41
1-Si <sub>3</sub> H <sub>6</sub> B	-872.05920	-872.12692	1.84		Si <sub>6</sub> H <sub>8</sub> A	-1741.82408	-1741.89592	1.96
2-Si <sub>3</sub> H <sub>6</sub> B	-872.05911	-872.13534	2.07		Si <sub>6</sub> H <sub>8</sub> B	-1741.82753	-1741.89836	1.93
Si <sub>3</sub> H <sub>5</sub>	-871.45601	-871.53701	2.20		Si <sub>6</sub> H <sub>7</sub>	-1741.21898	-1741.31098	2.50
Si <sub>3</sub> H <sub>4</sub> A	-870.84952	-870.90864	1.61		Si <sub>6</sub> H <sub>6</sub> A	-1740.62775	-1740.69673	1.88
Si <sub>3</sub> H <sub>4</sub> B	-870.84507	-870.92126	2.07		Si <sub>6</sub> H <sub>6</sub> B	-1740.63978	-1740.69004	1.37
1- <i>i</i> -Si <sub>4</sub> H <sub>9</sub>	-1163.38685	-1163.46535	2.14		1-Si <sub>7</sub> H <sub>15</sub>	-2035.52772	-2035.61350	2.33
2- <i>i</i> -Si <sub>4</sub> H <sub>9</sub>	-1163.39367	-1163.48031	2.36		2-Si <sub>7</sub> H <sub>15</sub>	-2035.53577	-2035.63002	2.56
1- <i>n</i> -Si <sub>4</sub> H <sub>9</sub>	-1163.38605	-1163.46368	2.11		Si <sub>7</sub> H <sub>14</sub> A	-2034.93125	-2035.00087	1.89
2- <i>n</i> -Si <sub>4</sub> H <sub>9</sub>	-1163.38891	-1163.47204	2.26		Si <sub>7</sub> H <sub>14</sub> B	-2034.91461	-2034.99405	2.16
1- <i>i</i> -Si <sub>4</sub> H <sub>8</sub> A	-1162.78971	-1162.85128	1.68		Si <sub>7</sub> H <sub>13</sub>	-2034.35723	-2034.45150	2.57
1- <i>n</i> -Si <sub>4</sub> H <sub>8</sub> A	-1162.78376	-1162.84397	1.64		Si <sub>7</sub> H <sub>12</sub> A	-2033.75810	-2033.82753	1.89
2- <i>n</i> -Si <sub>4</sub> H <sub>8</sub> A	-1162.78897	-1162.85054	1.68		Si <sub>7</sub> H <sub>12</sub> B	-2033.73948	-2033.81760	2.13
1- <i>i</i> -Si <sub>4</sub> H <sub>8</sub> B	-1162.77513	-1162.84720	1.96		Si <sub>7</sub> H <sub>11</sub>	-2033.16296	-2033.25530	2.51
1- <i>n</i> -Si <sub>4</sub> H <sub>8</sub> B	-1162.77134	-1162.84245	1.94		Si <sub>7</sub> H <sub>10</sub> A	-2032.56478	-2032.62468	1.63
2- <i>n</i> -Si <sub>4</sub> H <sub>8</sub> B	-1162.77359	-1162.85362	2.18		Si <sub>7</sub> H <sub>10</sub> B	-2032.55460	-2032.63020	2.06
Si <sub>4</sub> H <sub>7</sub>	-1162.19508	-1162.27396	2.15		Si <sub>7</sub> H <sub>9</sub>	-2031.95704	-2032.05117	2.56
Si <sub>4</sub> H <sub>6</sub> A	-1161.59921	-1161.65186	1.43		Si <sub>7</sub> H <sub>8</sub> A	-2031.33803	-2031.42173	2.28
Si <sub>4</sub> H <sub>6</sub> B	-1161.58112	-1161.65844	2.10		Si <sub>7</sub> H <sub>8</sub> B	-2031.36086	-2031.42546	1.76
Si <sub>5</sub> H <sub>11</sub>	-1454.10206	-1454.18453	2.24		Si <sub>7</sub> H <sub>7</sub>	-2030.74194	-2030.83444	2.52
1-Si <sub>5</sub> H <sub>10</sub> A	-1453.49791	-1453.56115	1.72		Si <sub>7</sub> H <sub>6</sub> A	-2030.12875	-2030.19854	1.90
2-Si <sub>5</sub> H <sub>10</sub> A	-1453.50696	-1453.57307	1.80		Si <sub>7</sub> H <sub>6</sub> B	-2030.13432	-2030.20358	1.88

<sup>a</sup> Total energy at the B3LYP/6-311+G(3df,2p)//B3LYP/6-31G(d) level including zero point energy computed from the vibrational frequencies at the B3LYP/6-31G(d) level, scaled by 0.9613. <sup>b</sup> From Perrin et al.<sup>4</sup>

the “A” suffix indicates a silene, and the “B” suffix indicates a silylene. For the few species with experimentally known electron affinities, the agreement between calculated and experimental results is excellent. All of the unsaturated silicon species are predicted to form stable anions in the gas phase. The silyl radicals, for whom the addition of an electron leads to a closed-shell electronic structure, have the largest electron affinities, ranging from 1.4 eV for SiH<sub>3</sub> to about 2.5 eV for the clusters containing seven silicon atoms. Electron affinities for the silylene biradicals are slightly smaller, ranging from 1.2 eV for SiH<sub>2</sub> to 2.3 eV for Si<sub>6</sub>H<sub>10</sub>. Electron affinities for the silenes are slightly smaller yet.

For each of the three types of compound, the electron affinity systematically increases with cluster size. This is illustrated in Figure 2, which shows the electron affinities of the acyclic terminal silyl, silylene, and silene species. For these acyclic structures with terminal functional groups, the increase in electron affinity with cluster size is well represented by the (purely empirical) functional form  $EA \text{ (eV)} = a - b(n_{\text{Si}})^c$ , where EA is the adiabatic electron affinity, and  $n_{\text{Si}}$  is the number of silicon atoms in the cluster. For the acyclic terminal silyl radicals,  $a = 3.42 \text{ eV}$ ,  $b = 2.00 \text{ eV}$ , and  $c = -0.314$ . For the acyclic terminal silenes,  $a = 3.36 \text{ eV}$ ,  $b = 2.45 \text{ eV}$ , and  $c = -0.256$ . For the acyclic terminal silylenes,  $a = 2.74 \text{ eV}$ ,  $b = 1.58 \text{ eV}$ , and  $c = -0.518$ . These curves are shown along with the calculated electron affinities in Figure 2. These empirical functions provide a reasonable means of estimating the electron affinities of slightly larger structures.

For the silyl radicals, the electron affinity increases with substitution of silyl groups for H at the radical site. The acyclic secondary silyl radicals, 2-Si<sub>3</sub>H<sub>7</sub>, 2-*n*-Si<sub>4</sub>H<sub>9</sub>, and 2-Si<sub>6</sub>H<sub>13</sub>, have electron affinities that are greater than the corresponding primary radicals, 1-Si<sub>3</sub>H<sub>7</sub>, 1-*n*-Si<sub>4</sub>H<sub>9</sub>, and 1-Si<sub>6</sub>H<sub>13</sub>, by 0.16, 0.15, and 0.17 eV, respectively. The acyclic tertiary silyl radicals, 2-*i*-Si<sub>4</sub>H<sub>9</sub> and 2-Si<sub>7</sub>H<sub>15</sub>, have electron affinities that are greater than the corresponding primary radicals, 1-*i*-Si<sub>4</sub>H<sub>9</sub> and 1-Si<sub>7</sub>H<sub>15</sub>, by 0.22 and 0.23 eV, respectively. The same effect is seen for the silylene biradicals. The acyclic secondary silylenes, 2-Si<sub>3</sub>H<sub>6</sub> and 2-*n*-Si<sub>4</sub>H<sub>8</sub>B, have electron affinities that are higher than the corresponding primary silylenes, 1-Si<sub>3</sub>H<sub>6</sub> and 1-*n*-Si<sub>4</sub>H<sub>8</sub>B, by 0.23 and 0.24 eV, respectively. This effect is much smaller, though still present, for the silenes. The electron affinity of 2-*n*-Si<sub>4</sub>H<sub>8</sub>A, with two silyl substituents is only 0.04 eV higher than that of 1-*n*-Si<sub>4</sub>H<sub>8</sub>A, which has only one silyl substituent. Similarly, 2-Si<sub>5</sub>H<sub>10</sub>A, with three silyl substituents has an electron affinity that is 0.08 eV greater than that of 1-Si<sub>5</sub>H<sub>10</sub>A, which has only one silyl substituent. The above observations can be generalized as follows. The electron affinity of unsaturated silicon–hydrogen molecules increases with silyl substitution for hydrogen at the unsaturated site. The electron affinity of secondary silyl radicals is about 0.16 eV greater than that of primary silyl radicals, while the electron affinity of tertiary silyl radicals is about 0.22 eV greater than that of primary silyl radicals. The electron affinity of secondary silylenes is about 0.23 eV greater than that of primary silylenes. The electron affinity of silenes increases by about 0.04 eV for each substitution of silyl for hydrogen.

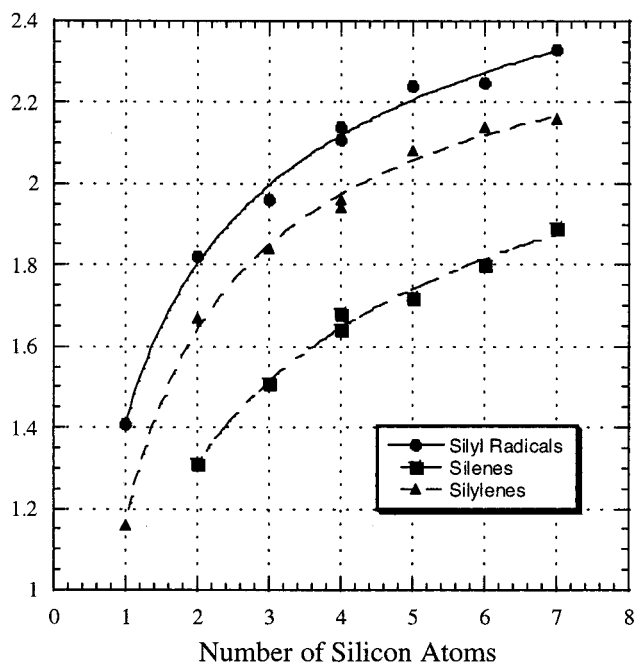


**Figure 2.** Changes in electron affinity with cluster size for acyclic terminal silyl radicals ( $\text{SiH}_3$ ,  $\text{H}_3\text{SiSiH}_2$ ,  $1\text{-Si}_3\text{H}_7$ ,  $1\text{-}i\text{-Si}_4\text{H}_9$ ,  $1\text{-}n\text{-Si}_4\text{H}_9$ ,  $\text{Si}_5\text{H}_{11}$ ,  $1\text{-Si}_6\text{H}_{13}$ , and  $1\text{-Si}_7\text{H}_{15}$ ), acyclic terminal silenes ( $\text{H}_2\text{SiSiH}_2$ ,  $\text{Si}_3\text{H}_6\text{A}$ ,  $1\text{-}i\text{-Si}_4\text{H}_8\text{A}$ ,  $1\text{-}n\text{-Si}_4\text{H}_8\text{A}$ ,  $1\text{-Si}_5\text{H}_{10}\text{A}$ ,  $\text{Si}_6\text{H}_{12}\text{A}$ ,  $\text{Si}_7\text{H}_{14}\text{A}$ ), and acyclic terminal silylenes ( $\text{SiH}_2$ ,  $\text{H}_3\text{SiSiH}$ ,  $1\text{-Si}_3\text{H}_6\text{B}$ ,  $1\text{-}i\text{-Si}_4\text{H}_8\text{B}$ ,  $1\text{-}n\text{-Si}_4\text{H}_8\text{B}$ ,  $\text{Si}_5\text{H}_{10}\text{B}$ ,  $\text{Si}_6\text{H}_{12}\text{B}$ ,  $\text{Si}_7\text{H}_{14}\text{B}$ ). Points are individual calculations, lines are fits to the functional form  $\text{EA (eV)} = a - b(n_{\text{Si}})^c$ , where EA is the adiabatic electron affinity and  $n_{\text{Si}}$  is the number of silicon atoms in the cluster. For the acyclic terminal silyl radicals,  $a = 3.42$  eV,  $b = 2.00$  eV, and  $c = -0.314$ . For the acyclic terminal silenes,  $a = 3.36$  eV,  $b = 2.45$  eV, and  $c = -0.256$ . For the acyclic terminal silylenes,  $a = 2.74$  eV,  $b = 1.58$  eV, and  $c = -0.518$ .

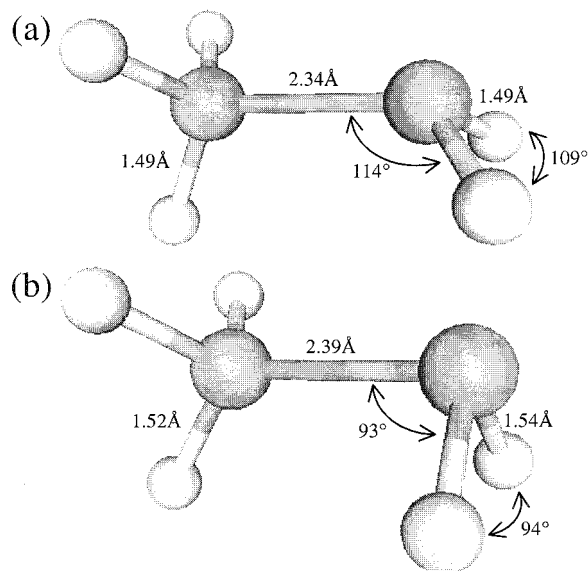


**Figure 3.** Geometric changes in going from the neutral silyl radical  $\text{H}_3\text{SiSiH}_2$  (a) to the corresponding anion (b).

The typical differences in molecular geometry between the neutral species and their corresponding anions are illustrated in Figures 3–5. Upon addition of an electron, the silyl radicals show a slight lengthening of all of the bonds near the radical site, and a substantial decrease in the bond angles at the radical site. For  $\text{H}_3\text{SiSiH}_2$ , shown in Figure 3, the Si–Si–H and H–Si–H bond angles at the radical site decrease from  $114^\circ$

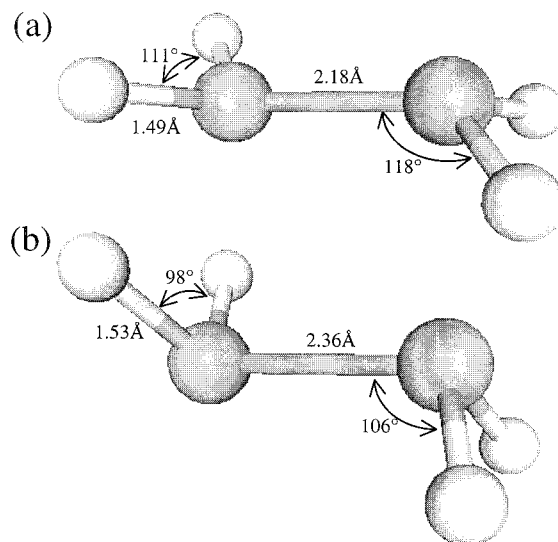


**Figure 4.** Geometric changes in going from the neutral silene (a) to the corresponding anion (b).

and  $109^\circ$  in the neutral molecule to  $94^\circ$  and  $93^\circ$  in the anion. In this case, the addition of an electron fills the partially filled nonbonding  $\text{sp}^3$  orbital of the silicon atom, and the resulting high electron density and negative electrostatic potential “push” the other atoms away. A similar difference in geometry between the neutral and the anion is observed for the silenes. The atoms attached to the nominally double-bonded silicon atoms in silenes are nearly coplanar, and there is weak  $\pi$  bonding between the two nominally double-bonded silicon atoms. Addition of an electron disrupts this  $\pi$  bonding, and as a result the anion is much further from being planar. This change in geometry was computed and described by Kalcher and Sax.<sup>13</sup> This is shown for  $\text{H}_2\text{SiSiH}_2$  in Figure 4, where the Si–Si–H and H–Si–H bond angles go from  $118^\circ$  and  $111^\circ$  in the neutral molecule to  $106^\circ$  and  $98^\circ$  in the anion. At the same time, the nominal double bond lengthens from 2.18 to 2.36 Å, a value typical of a Si–Si single bond. Such a difference in geometry between the neutral molecule and the anion is not observed for the silylenes. As shown in Figure 5 for  $\text{H}_3\text{SiSiH}$ , there are slight differences in bond lengths and almost no differences in bond angles between the neutral silylene and the corresponding anion.

For the most part, the electron affinities of the cyclic and polycyclic structures are consistent with and follow the same trends as the acyclic molecules discussed above. Deviations from the behavior of the acyclic molecules arise from (a) differences in ring strain between the neutral molecule and the anion or (b) differences in the interactions between nonbonding electrons and other atoms between the neutral molecule and the anion. The effect of changes in ring strain between the neutral molecule and the corresponding anion is well illustrated by  $\text{Si}_3\text{H}_5$ ,  $\text{Si}_3\text{H}_4\text{A}$ , and  $\text{Si}_3\text{H}_4\text{B}$ . For  $\text{Si}_3\text{H}_5$ , the electron affinity is slightly higher than the electron affinity of  $2\text{-Si}_3\text{H}_7$ , even though they are both secondary silyl radicals and both contain three silicon atoms. This can be rationalized by noting that constraining the three silicon atoms into a three-membered ring causes less strain for the anion than the neutral, because the bond angles in the unstrained anion would be smaller than those in the unstrained neutral molecule. Since the anion requires less strain energy to form the ring, it is stabilized relative to the neutral, and the electron affinity is increased. Likewise,  $\text{Si}_3\text{H}_4\text{A}$  has a larger electron affinity than  $\text{Si}_3\text{H}_6\text{A}$ . Again, the bond angles of the anion are naturally smaller than those of the neutral, so the anion has less ring strain energy than the neutral molecule, and the



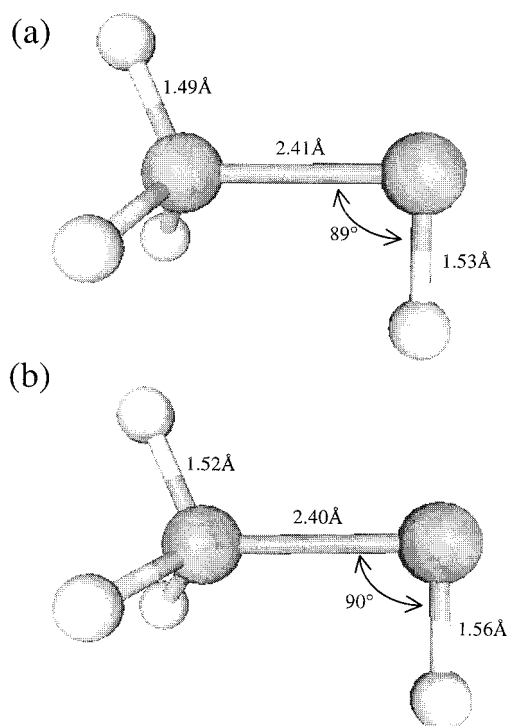


**Figure 5.** Geometric changes in going from the neutral silylene (a) to the corresponding anion (b).

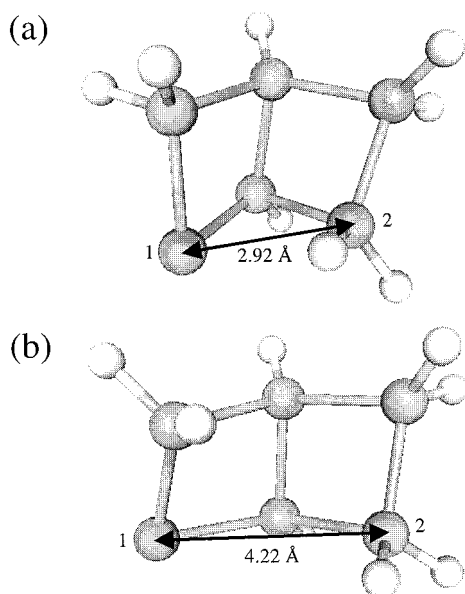


**Figure 6.** Structures of (a) neutral and (b) anionic Si<sub>6</sub>H<sub>8</sub>B.

electron affinity is increased relative to our expectations. By contrast to these two cases, the electron affinity of Si<sub>3</sub>H<sub>4</sub>B is exactly the same as that of 2-Si<sub>3</sub>H<sub>6</sub>B, as we would expect. Since the geometry of the neutral silylenes and their anions are almost identical, there is no significant difference in the ring strain energy between the neutral molecule and the anion. For some of the polycyclic structures, deviations of the electron affinity from its expected value appears to arise from differences in interactions between nonbonding electrons and other atoms for the neutral molecule and the anion. An example of this is given by Si<sub>6</sub>H<sub>8</sub>B, for which the structures of the neutral molecule and the anion are shown in Figure 6. In the neutral molecule, there is a substantial interaction between the silylene group (labeled "1" in Figure 6) and the silicon atom labeled "2" in Figure 6.

The distance between these two atoms is only 2.92 Å in the neutral molecule. Addition of an electron disrupts this interaction, and in the anion the distance between these two atoms is 4.22 Å. Thus, the interaction between the silylene group and silicon atom "2" stabilizes the neutral relative to the anion, lowering the electron affinity. This same effect, in even greater degree, is seen for Si<sub>6</sub>H<sub>6</sub>B. Unfortunately, while we can rationalize these deviations from the expected values of electron affinity based on the acyclic compounds, we cannot quantitatively predict these deviations. Thus, for cyclic and polycyclic clusters where these deviations may be expected to arise, we cannot reliably estimate the electron affinity based on the trends presented above but must perform a more detailed calculation.

## Summary and Conclusions

Adiabatic electron affinities for 72 hydrogenated silicon compounds containing up to seven silicon atoms have been presented. These were computed using density functional theory at the B3LYP/6-311+G(3df,2p)/B3LYP/6-31G(d) level and are expected to be accurate to within about 0.15 eV. The electron affinities for acyclic silyl radicals, silylenes, and silenes were all found to increase smoothly with increasing molecular size. Electron affinities of the silyl radicals were greater than those of the silylenes, which were, in turn, greater than those of the silenes. Electron affinities increased with silyl substitution for hydrogen at the unsaturated site for all three of these classes of compounds. Some cyclic and polycyclic clusters had electron affinities that deviated significantly from the trends observed for the acyclic compounds. These deviations could be rationalized in terms of differences in ring strain between the neutral and anionic species and in terms of differences in the interactions between nonbonding electrons and other atoms between the neutral and anionic species.

**Acknowledgment.** This work was partially supported by generous grants of supercomputer resources from the Supercomputer Institute of the University of Minnesota and from the Center for Computational Research of the University at Buffalo (SUNY). Valuable conversations with and encouragement from Steven Girshick, Uwe Kortshagen, and Upendra Bhandarkar of the University of Minnesota are also gratefully acknowledged.

## References and Notes

- (1) Girshick, S. L.; Swihart, M. T.; Suh, S.-M.; Mahajan, M. R.; Nijhawan, S. *Proc. Electrochem. Soc.* **1999**, 98-23, 215.
- (2) Swihart, M. T.; Girshick, S. L. *J. Phys. Chem. B* **1999**, 103, 64.
- (3) Kortshagen, U. R.; Bhandarkar, U. V.; Swihart, M. T.; Girshick, S. L. *Generation and Growth of Nanoparticles in Low-Pressure Plasmas*, 14th International Symposium on Plasma Chemistry, 1999, Institute of Plasma Physics, Prague, Czech Republic (to appear in *Pure Appl. Chem.*).
- (4) Perrin, J.; Leroy, O.; Bordage, M. C. *Contrib. Plasma Phys.* **1996**, 36, 3.
- (5) Kalcher, J.; Sax, A. F. *Chem. Rev.* **1994**, 94, 2291.
- (6) Damrauer, R.; Hankin, J. A. *Chem. Rev.* **1995**, 95, 1137.
- (7) Becke, A. D. *Phys. Rev. A* **1988**, 38, 3098.
- (8) Lee, C.; Yang, W.; Parr, R. G. *Phys. Rev. B* **1988**, 37, 785.
- (9) Becke, A. D. *J. Chem. Phys.* **1993**, 98, 5648.
- (10) Wong, M. W. *Chem. Phys. Lett.* **1996**, 256, 391.
- (11) Frisch, M. J.; Trucks, G. W.; Schlegel, H. B.; Gill, P. M. W.; Johnson, B. G.; Robb, M. A.; Cheeseman, J. R.; Keith, T.; Petersson, G. A.; Montgomery, J. A.; Raghavachari, K.; Al-Laham, M. A.; Zakrzewski, V. G.; Ortiz, J. V.; Foresman, J. B.; Cioslowski, J.; Stefanov, B. B.; Nanayakkara, A.; Challacombe, M.; Peng, C. Y.; Ayala, P. Y.; Chen, W.; Wong, M. W.; Andres, J. L.; Replogle, E. S.; Gomperts, R.; Martin, R. L.; Fox, D. J.; Binkley, J. S.; Defrees, D. J.; Baker, J.; Stewart, J. P.; Head-Gordon, M.; Gonzalez, C.; Pople, J. A. *Gaussian 94*, revision D.4; Gaussian, Inc.: Pittsburgh, PA, 1995.
- (12) Curtiss, L. A.; Redfern, P. C.; Raghavachari, K.; Pople, J. A. *J. Chem. Phys.* **1998**, 109, 42.
- (13) Kalcher, J.; Sax, A. F. *Chem. Phys. Lett.* **1992**, 192, 451.